Singlet magnetism in intermetallic UGa_2 unveiled by inelastic x-ray scattering

Andrea Marino,[1] Martin Sundermann,[1,2] Denise S. Christovam,[1] Andrea Amorese,[1,3,*] Chun-Fu Chang,[1] Paulius Dolmantas,[1] Ayman H. Said,[4] Hlynur Gretarsson,[2] Bernhard Keimer,[5] Maurits W. Haverkort,[6] Alexander V. Andreev,[7] Ladislav Havela,[8] Peter Thalmeier,[1] Liu Hao Tjeng,[1] and Andrea Severing[1,3]

[1]*Max Planck Institute for Chemical Physics of Solids, Nöthnitzer Straße 40, 01187 Dresden, Germany*
[2]*PETRA III, Deutsches Elektronen-Synchrotron DESY, Notkestraße 85, 22607 Hamburg, Germany*
[3]*Institute of Physics II, University of Cologne, Zülpicher Str. 77, 50937 Cologne, Germany*
[4]*Advanced Photon Source, Argonne National Laboratory, 9700 S Cass Ave, Lemont, Illinois 60439, USA*
[5]*Max Planck Institute for Solid State Research, Heisenbergstraße 1, D-70569 Stuttgart, Germany*
[6]*Institute for Theoretical Physics, Heidelberg University, Philosophenweg 19, 69120 Heidelberg, Germany*
[7]*Institute of Physics, Academy of Sciences of the Czech Republic, Na Slovance 1999/2, 182 21 Prague 8, Czech Republic*
[8]*Department of Condensed Matter Physics, Faculty of Mathematics and Physics, Charles University, Ke Karlovu 5, 121 16 Prague 2, Czech Republic*

(Received 3 March 2023; revised 30 May 2023; accepted 14 July 2023; published 27 July 2023)

Using high resolution tender x-ray resonant inelastic scattering and hard x-ray nonresonant inelastic scattering beyond the dipole limit we were able to detect electronic excitations in intermetallic UGa_2 that are highly atomic in nature. Analysis of the spectral lineshape reveals that the local $5f^2$ configuration characterizes the correlated nature of this ferromagnet. The orientation and directional dependence of the spectra indicate that the ground state is made of the Γ_1 singlet and/or Γ_6 doublet symmetry. With the ordered moment in the *ab* plane, we infer that the magnetism originates from the higher lying Γ_6 doublet being mixed with the Γ_1 singlet due to intersite exchange, qualifying UGa_2 to be a true quantum magnet. The ability to observe atomic excitations is crucial to resolve the ongoing debate about the degree of localization versus itineracy in U intermetallics.

DOI: 10.1103/PhysRevB.108.045142

I. INTRODUCTION

Actinide intermetallics show a wealth of fascinating phenomena that includes heavy-fermion behavior, hidden order or unconventional magnetism, unconventional superconductivity, the combination of ferromagnetism and superconductivity [1–3], orbital multicomponent [4], or spin-triplet superconductivity [5–8] with unusual topological properties [9]. It is generally understood that those complex emergent properties originate from the intricate interplay of band formation and correlations involving the $5f$ electrons. It is, however, far from clear how to describe quantitatively the electronic structure of these systems, for example, whether an itinerant approach [2,3] or an embedded impurity model which includes explicitly the local degrees of freedom [10–12] would be the better starting point. The main problem is that many intermetallic uranium compounds, perhaps with the exception of UPd_3 [13,14], do not exhibit excitations in their inelastic neutron scattering data. It is therefore challenging to understand if remnants of atomiclike states are at all present in these compounds, let alone to pinpoint which multiplet and/or crystal-field state is actually occupied.

Here we investigate UGa_2 as a representative case for many metallic U compounds in which the relative importance between itinerancy and localization is at issue in explaining the physical properties. UGa_2 crystallizes in the hexagonal AlB_2 structure (space group P6/*mmm*) [15], with the U-U distances well above the Hill limit [16], and orders ferromagnetically below $T_c = 125$ K with a small orthorhombic distortion [17]. The moments are aligned in the *ab* plane along the *a* crystallographic direction. The size of the uranium moment as determined by neutron diffraction [18] and magnetization [19–21] measurements amounts to about $3\,\mu_B$, quite a high value as compared to other magnetically ordered uranium intermetallics, and suggests a more localized nature of the $5f$ states in this binary. Inelastic neutron scattering, however, did not find crystal-field excitations; only magnons below 10 meV were observed [22]. Attempts to explain the magnetism have been based on local f^2 and f^3 charge configurations [20,23–25], and on approaches that include itinerancy [24,26]. De Haas–van Alphen [20] and photoemission [27,28] experiments indicate that UGa_2 is neither localized nor itinerant. Spectroscopically, photoemission experiments are also not conclusive: core level data on bulk samples were interpreted as indicative for the localized nature of the $5f$ states, based on the satellite structure of the U $4f$ core level that looks

*ASML Netherlands B.V., De Run 6501, 5504 DR, Veldhoven, The Netherlands.

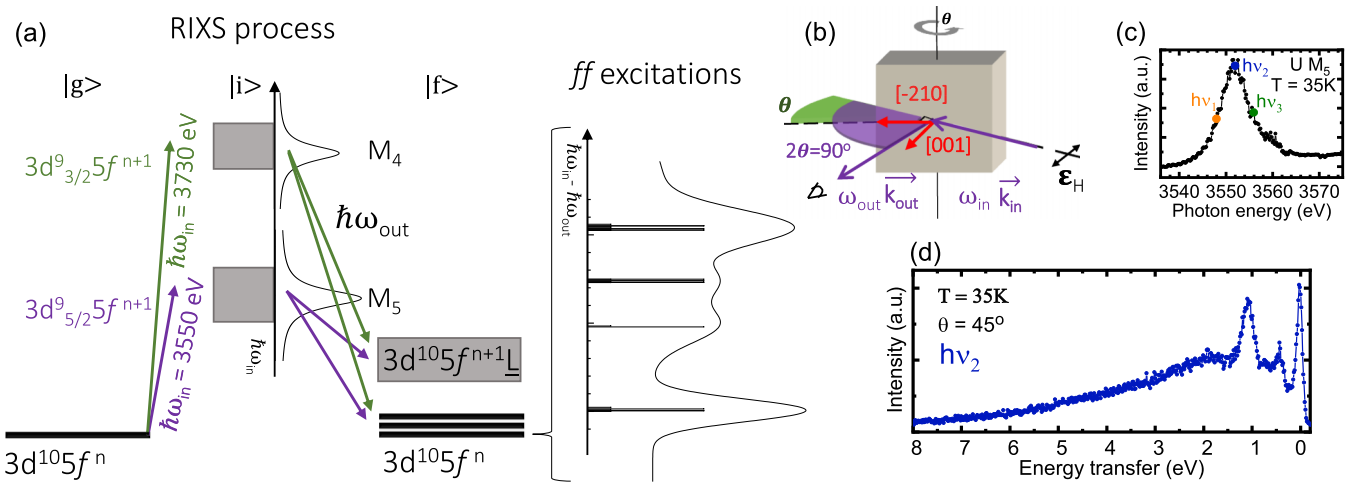

FIG. 1. (a) RIXS process at the U $M_{4,5}$ edge for a $5f^n$ ground state. (b) Scattering geometry of the RIXS experiment. The scattering angle is kept at $2\Theta = 90^\circ$. (c) Fluorescence-yield M_5 XAS spectrum of UGa_2. Large dots mark the photon energies where RIXS is measured ($h\nu_1$, $h\nu_2$, and $h\nu_3$). (d) M_5 RIXS spectrum of UGa_2 acquired at $h\nu_2$ and $\theta = 45^\circ$.

very different from that of itinerant UB_2 [27,29]. On the other hand, data on UGa_2 films [30] seem to support itinerancy, based on the fact that the satellites appear at different energy positions than in prototypical UPd_3.

The observation of multiplets would provide direct evidence of the presence of atomiclike states. Furthermore, multiplets are a unique fingerprint of the configuration that determines the symmetry. Here, resonant inelastic x-ray scattering (RIXS) is the ideal method because it covers a wide range of energy transfers. Already in 2006, Kvashnina *et al.* and Burotin *et al.* used RIXS at the U *O* edge (≈100 eV) to distinguish valence states in semiconducting UO_2 and other U and actinide oxides [31–33], and Wray *et al.* and Liu *et al.* reported excitations in the *O*-edge RIXS spectra of intermatallic U compounds [34,35]. However, the signal to background ratio of these f-f excitations is very small at the U *O* edge because of the strong elastic tail in the extreme ultraviolet. A recent publication of soft RIXS data at the U N_4 edge (≈778 eV), also of UO_2 [36], encouraged some of the authors of this manuscript to repeat the N_4-edge experiment with the same experimental setup for the intermetallic large moment antiferromagnet UNi_2Si_2. The result was discouraging, with absolutely no inelastic intensity observed [37]. Another trial at the N_5 edge (≈736 eV) of the hidden order compound URu_2Si_2 gave the same negative result [38]. Kvashnina *et al.*, on the other hand, reported tender x-ray RIXS experiments at the U M_4 (≈3730 eV) and M_5 (≈3552 eV) edge with a resolution of 1 eV for UO_2, and for the two intermetallic compounds UPd_3 and URu_2Si_2. Distinct excitations are observed at about 3−7 eV (valence band into unoccupied $5f$ states) and 18−20 eV (U $5f$ to U $6p$), both at the M_4 and M_5 edge [39]. These data show that the realization of *high-resolution tender* RIXS at the U *M* edges is the most promising direction to aim at, not only because of the expected stronger signal, but also because the tender x-ray regime does not require cleaving; it would even allow the confinement of samples. The latter would be a great advantage when performing experiments on U and especially actinide containing samples.

Here we utilize this new spectroscopic tool, namely *high-resolution tender* RIXS at the U M_5 edge to tackle the origin of the magnetism in UGa_2. With tender RIXS, we were able to detect pronounced atomic multiplet states in the intravalence band excitation spectrum of UGa_2. We also present hard x-ray core-level nonresonant inelastic scattering data (NIXS, also known as x-ray Raman) in the beyond-dipole limit at the U $O_{4,5}$ edge, confirming the RIXS result. Also in the high energy NIXS spectrum we observed states that are highly atomic in nature. Our analysis ultimately indicates that UGa_2 is a singlet ferromagnet.

II. METHODS

A. High resolution tender RIXS at U M_5-edge

In a U $M_{4,5}$-edge RIXS experiment, see Fig. 1(a), a $3d$ core electron is excited from the $3d^{10}5f^n$ ground state $|g\rangle$ into the $5f$ shell by the absorption of incoming photons at the M_5 (3552 eV) or M_4 (3730 eV) edge, leading to $3d^9_{5/2}5f^{n+1}$ or $3d^9_{3/2}5f^{n+1}$ intermediate states $|i\rangle$, respectively. The subsequent de-excitation of the $3d$ core can be into the ground state (elastic peak), into an excited state of the same local charge configuration (ff excitations, phonons, magnons) [40–43], or into an excited state of a different charge configuration (charge transfer excitations) [44–46].

Figure 1(b) depicts the experimental geometry where the scattering angle is set at $2\Theta = 90^\circ$ to minimize the elastic intensity. The UGa_2 samples used for the experiments were grown with the Czochralski method [21] and their surface is the *ab* plane, i.e., it has the [001] orientation.

High resolution tender RIXS was performed at the Max-Planck RIXS end station (IRIXS) of the P01 beamline at Petra III/DESY in Hamburg. The instrument is unique, since it allows to perform RIXS experiments with tender x-rays (2.5–3.5 keV) and good resolution [47]. For example, a resolution of 100 meV can be achieved at the Ru L_3 edge at 2840 eV. The IRIXS beamline uses the hard x-ray set-up

[47]. For the U M_5 edge at 3550 eV a diced quartz waver (112), pressed and glued on a concave Si lens, has been used as analyzer crystal [48]. The instrument 150 meV Gaussian response function at the U M_5 edge is estimated by measuring a carbon tape. The experiment was performed with horizontal polarization of the the incident photons, a scattering angle $2\Theta = 90^\circ$ to minimize elastic intensity and sample angles of $\theta = 20^\circ, 45^\circ$, and 80° [see Fig. 1(b)]. Temperature was kept at 35 K.

B. NIXS with hard x-rays at U $O_{4,5}$ edge

NIXS with hard x-rays (10 keV) and large momentum transfer is dominated by higher-than-dipole transitions [49,50], which are more excitonic in contrast to the dipole contribution [51–54]. The direction of the momentum transfer $\vec{q}$ in NIXS plays an analogous role as the electric field vector $\vec{E}$ in XAS and is sensitive to the symmetry of the crystal-field ground state.

The experiments are performed at the Max-Planck NIXS end stations of the P01 beamline at Petra III/DESY in Hamburg. A sketch and description of the NIXS experimental setup is shown in Fig. 2 of Ref. [55]. 10 keV photons are used. The average scattering angle 2Θ at which the analyzers are positioned is $\approx 150^\circ$, thus yielding a momentum transfer of $|\vec{q}| = (9.6 \pm 0.1)\,\text{Å}^{-1}$ at elastic scattering. An instrumental energy resolution of about 0.8 eV FWHM is achieved. The sample is kept in a vacuum cryostat at $T = 5\,\text{K}$. The $O_{4,5}$ edge of U is measured with momentum transfer $\vec{q}$ parallel to the a and c crystallographic directions.

III. RESULTS

Figure 1(c) shows the experimental U M_5-edge x-ray absorption (XAS) spectrum of UGa_2. The large dots mark the photon energies used in this RIXS study, $E_{\text{res}} - 4\,\text{eV}$ ($h\nu_1$), E_{res} ($h\nu_2$), and $E_{\text{res}} + 4\,\text{eV}$ ($h\nu_3$) with $E_{\text{res}} = 3552$ eV. In Fig. 1(d) the RIXS spectrum of UGa_2 is displayed for a wide energy range up to 8 eV energy transfer taken at the M_5 resonance ($h\nu_2$) with the sample angle of $\theta = 45^\circ$. The spectrum exhibits sharp peaks below 2 eV that are on top of a broad feature that arises most likely from charge transfer excitations. The sharp peaks are very typical of local atomiclike excitations.

Figure 2 shows a closeup of the first 2 eV of RIXS spectra that were measured with different incident energies, $h\nu_1$, $h\nu_2$, and $h\nu_3$. The data are normalized to the peak at 1.05 eV. The intensities of the peaks vary considerably with the incoming photon energy so that three inelastic excitations at 0.44, 0.70, and 1.05 eV can be identified. We assign these to intermultiplet ff transitions since the energies are too high for magnons and crystal-field excitations.

Full atomic multiplet calculations assuming a $5f^2$ and alternatively a $5f^3$ configuration were carried out to simulate the spectra. For this, the *Quanty* code [56] was used with the atomic values of the the spin-orbit constant and the $5f$-$5f$ and $3d$-$5f$ Slater integrals from the Atomic Structure Code by Robert D. Cowan [57] as input parameters, whereby the spin orbit constant was reduced by 10% and the Slater integrals by 45% in order to take configuration interaction effects and covalence into account [58–60]. These are typical

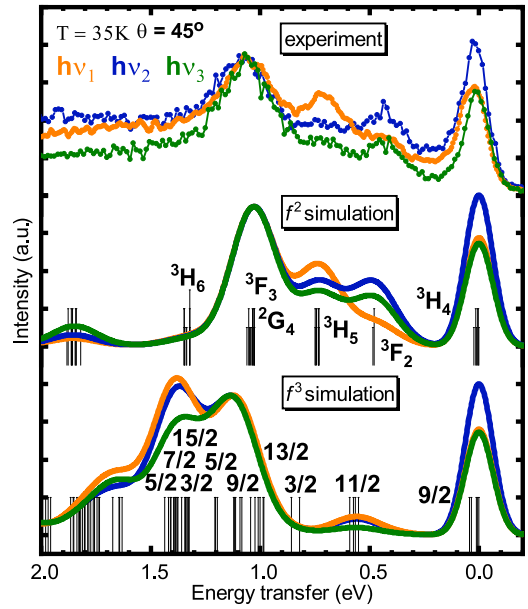

FIG. 2. M_5 RIXS spectra of UGa_2 acquired at $h\nu_1$, $h\nu_2$, and $h\nu_3$ with a sample angle $\theta = 45^\circ$ as compared to simulations using an $5f^2$ and $5f^3$ configuration.

reduction factors for uranium compounds [36]. A crystal-field (CF) potential was always considered. CF parameters were taken from fits to the magnetic susceptibility or magnetization, for the $5f^2$ from Ref. [25] and for the $5f^3$ configuration from Refs. [20,23], or constructed to test different CF ground state wave functions. Furthermore, a Lorentzian broadening of about 6 eV in the intermediate state was used, based on the width of the M_5 XAS spectrum, and a Gaussian broadening of 150 meV to account for the experimental resolution.

Figure 2 also shows the simulation for the $5f^2$ and for the $5f^3$ configuration. The calculation based on the $5f^2$ reproduces the experimental data in terms of peak positions as well as variation of the peak intensities with incident energy. The vertical lines represent the histogram of the multiplet states and provide a straightforward labeling of the peaks. The $5f^3$ simulation, on the other hand, does not reproduce the experimental data. It turns out that no matter how the reduction factors are tuned, an agreement cannot be achieved for $5f^3$ (see Appendix A 1). Hence, we conclude the atomiclike states in UGa_2 are given by the $5f^2$ configuration.

Next we determine the CF symmetry of the ground state. Here we ignore the slight orthorhombic distortion below T_c [17] since it is only a very small magnetostriction correction to the hexagonal crystal-field analysis. In D_{6h} the hexagonal CF splits the ninefold degenerate $J = 4$ Hund's rule ground state of the U $5f^2$ configuration into three singlets and three doublets. These can be written in the J_z representation as

$$\Gamma_1 = |0\rangle, \tag{1}$$

$$\Gamma_3 = \frac{1}{\sqrt{2}}|+3\rangle + \frac{1}{\sqrt{2}}|-3\rangle, \tag{2}$$

$$\Gamma_4 = \frac{1}{\sqrt{2}}|+3\rangle - \frac{1}{\sqrt{2}}|-3\rangle, \tag{3}$$

$$\Gamma_5^1 = \sin\phi|\pm 4\rangle + \cos\phi|\mp 2\rangle, \tag{4}$$

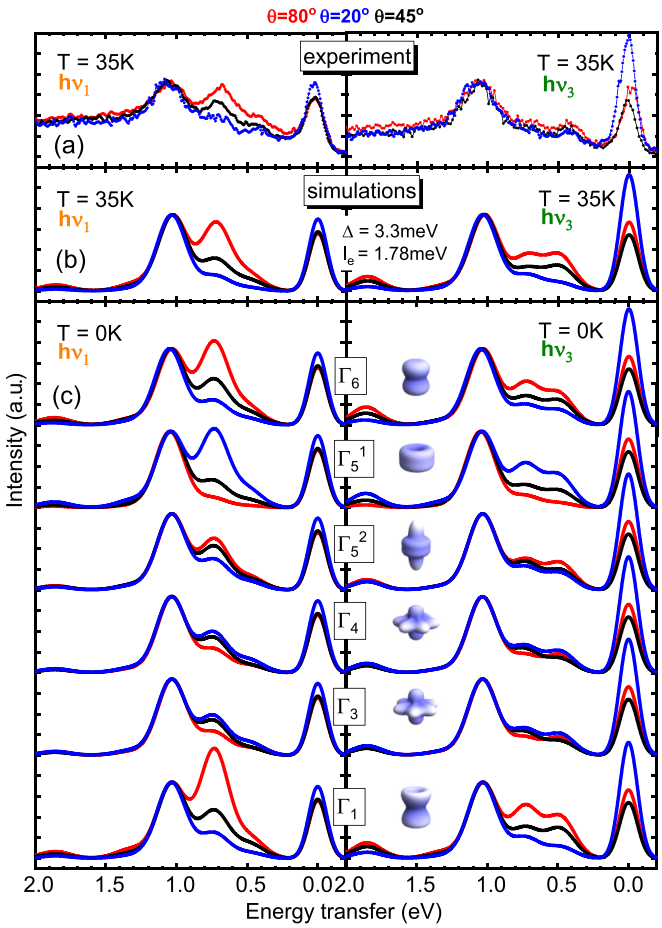

FIG. 3. (a) Experimental RIXS spectrum of UGa_2 acquired at $h\nu_1$ and $h\nu_3$ with sample angles $\theta = 80°$, 45°, and 20°. (b) Simulated 35 K RIXS spectra for an $5f^2$ configuration with the crystal-field parameters of Richter *et al.* [25] and a molecular field I_e of 1.78 meV. (c) Simulated 0 K RIXS spectra for each of the six crystal-field states of the $5f^2$.

$$\Gamma_5^2 = \cos\phi|\pm 4\rangle - \sin\phi|\mp 2\rangle, \quad (5)$$

$$\Gamma_6 = |\pm 1\rangle. \quad (6)$$

Although the CF splitting is below the resolution limit of the present RIXS experiment, it is possible to obtain information about the ground state symmetry by measuring the orientation dependence of the scattering signal [61]. The two panels of Fig. 3(a) show the RIXS spectra for two incident energies $h\nu_1$ and $h\nu_3$, whereupon each energy was measured for the three sample angles $\theta = 80°$, 45°, and 20°. The θ rotation is in the [001]-[-210] plane, see Fig. 1(b). The intensities are again normalized to the peak at 1.05 eV energy transfer. A pronounced orientation dependence can be seen in the spectra for $h\nu_1$, that has almost disappeared for $h\nu_3$.

Again the data are compared to the full multiplet calculations. In Fig. 3(b) we start with the calculations using the $5f^2$ crystal field parameters of Richter *et al.* [25]. With this set of parameters, the ground state is the Γ_1, the first excited state the Γ_6 at 3.3 meV, the second excited state the Γ_5^1 with $\sin\phi = 0.81$ at 5.9 meV, and all other states at 13 meV or higher. The calculations were performed for T=35 K and include a molecular field I_e of 1.78 meV as will be explained later. We observe that the calculations reproduce the experiment well: the simulation captures the strong orientation dependence for $h\nu_1$ in the correct sequence and its decrease for $h\nu_3$.

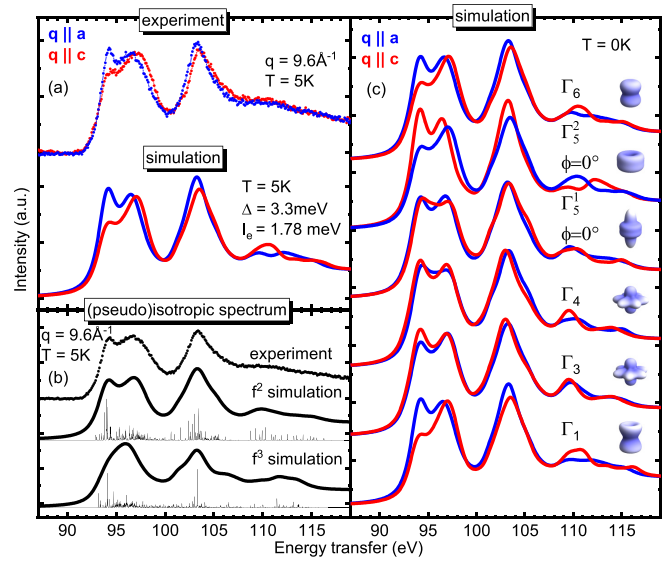

FIG. 4. (a) NIXS spectra for $\vec{q}||a$ and $\vec{q}||c$ together with the simulation using the crystal field parameters of Richter *et al.* [25] and a molecular field I_e of 1.78 meV. (b) (Pseudo)isotropic data and full multiplet simulations without crystal-field for the Uf^2 and Uf^3 configurations. (d) Simulated NIXS spectra for each of the six crystal-field states of the f^2 together with the corresponding charge densities.

To understand whether a different order of CF states would also be able to reproduce the experiment, we calculate the spectra for different CF ground states. To this end, we tuned slightly the CF parameters such that the desired CF state becomes the ground state and then we carried out the calculation for T=0 K. The results are displayed in Fig. 3(c). We observe that a Γ_1 ground state, or a Γ_6, or also a Γ_5^2 with $\cos\phi \approx 1$ have the correct trend in the orientation dependence for $h\nu_1$ and its reduction at $h\nu_3$. A Γ_3, Γ_4, or Γ_5^1 as ground state, on the other hand, produces an orientation dependence that is opposite to the experiment so that these three states can be excluded. The NIXS experiment below will show that also the Γ_5^2 cannot be the ground state. We thus conclude that the good simulation is based on the strong orientation dependence provided by the Γ_1 or the Γ_6 low lying states, which gets counteracted at 35 K by the Boltzmann occupation of a higher lying state with opposite orientation dependence, such as the Γ_5^1.

Figure 4(a) shows the $O_{4,5}$ edge NIXS data of UGa_2 at 5 K for $\vec{q}||c$ and $\vec{q}||a$, revealing a strong directional dependence. In Fig. 4(b) the (pseudo)isotropic U $O_{4,5}$ NIXS spectrum, constructed from $I_{\rm iso} = (I_{\mathbf{q}||c} + 2I_{\mathbf{q}||a})/3$, is displayed and compared to atomic simulations without considering the crystal-field Hamiltonian. The Slater integrals for the $5f$-$5f$ and $5d$-$5f$ Coulomb interactions are reduced by about 40% with respect to their atomic values. The value of the momentum transfer in the simulation is set to $|\vec{q}| = 11.1$ Å^{-1} in order to account for the U $5f$ radial wave

function in the solid being different from the calculated atomic value. An arctangent type of background is added to account for the edge jump. A Gaussian broadening of 0.8 eV and a Lorentzian broadening of 1.3 eV account for instrumental resolution and lifetime effects, respectively. The simulations are performed both for an $5f^2$ and $5f^3$ configuration and also here only the f^2 simulation reproduces the experimental lineshape, whereas the f^3 does not (see Appendix A 2). This finding is fully consistent with the RIXS results.

Focusing now on the directional dependence, we calculate the spectra for each of the six possible crystal-field states. The results are displayed in Fig. 4(c). Comparison with experiment immediately excludes the Γ_3 and Γ_4 singlets, as well as the Γ_5 doublets for any range of the parameter ϕ (see equations above). For the $\Gamma_5^{(1,2)}$ doublets only the extreme cases of $\phi = 0^o$ are shown, since the spectra for all other ϕ values fall between these two extremes. The Γ_1 singlet and the Γ_6 doublet, on the other hand, show the same directional dependence as the experiment, thus confirming the RIXS results.

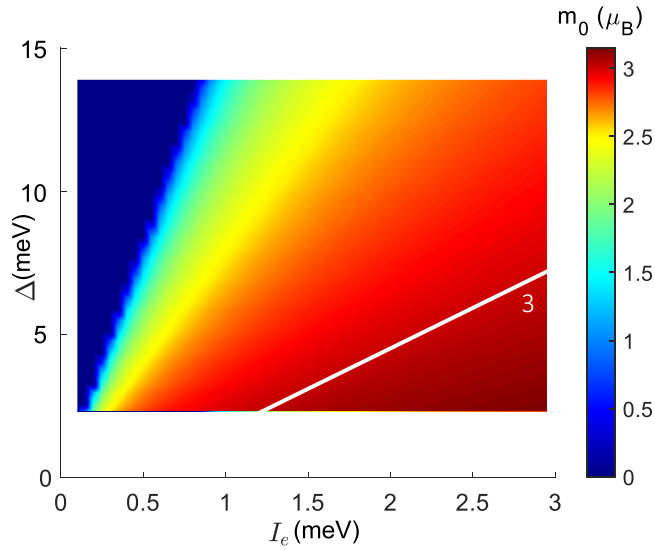

FIG. 5. Magnetic moment m_0 at zero temperature as a function of the Γ_1-Γ_6 splitting Δ and the effective exchange I_e. The white line denotes the contour with $m_0 = 3\ \mu_B$.

IV. DISCUSSION

The above NIXS and RIXS results find that the $5f^2$ configuration dominates the local electronic structure of UGa_2 and that the symmetry of the CF ground state is either given by the Γ_1 singlet and/or Γ_6 doublet. However, we can further exclude the Γ_6 doublet as ground state because it would yield an ordered moment along c and not in the ab plane. Hence, the Γ_1 singlet state must be the lowest one in energy. Yet, the Γ_6 is also a necessary ingredient for the magnetism in UGa_2 as we will discuss in the following.

In a conventional local moment magnet the nonvanishing temperature independent moments are present at each lattice site and then order spontaneously at the transition temperature creating a self-consistent molecular field. This is basically a classical concept modified only by the influence of semiclassical quantum fluctuations which reduce the size of the ordered moment by a modest amount. A Γ_1 ground state would not carry a local moment so that the semiclassical picture of magnetic order does not apply, it rather must be classified as a true quantum magnet where the creation of the local moments and their ordering appears spontaneously at T_c. This mechanism of induced magnetic order is caused by the nondiagonal mixing of Γ_1 with excited Γ_6 states due to the effective intersite exchange coupling that forms the true ground state superposition below the ordering temperature. Induced quantum magnetism in singlet ground state systems has been explored in d^4 transition metal [62,63] or $4f^2$ Pr materials (see Ref. [64] and references therein). In these cases the presence of multiplets is clear. Singlet magnetism is however rarely recognized in U compounds [64–68], where pinpointing the U $5f^2$ configuration is already challenging (see also Appendix A 4).

Looking at the simple structure of CF states, we realize that indeed Γ_6 is the only possible excited state that has nonvanishing mixing matrix elements $\langle\Gamma_1|J_x|\Gamma_6\rangle$ for the in-plane total angular momentum operators (not for J_z) so that there can be no coupling to any other state when we restrict to the Hilbert space of the ground state multiplet ($J = 4$). This explains naturally that the ordered moment must lie in the hexagonal plane and at the same time the anisotropy of the paramagnetic susceptibility. For the induced moment mechanism of magnetic order to work, i.e., to produce a finite ordering temperature, the effective exchange I_e must surpass a critical value. Here I_e is the Fourier transform $I(\mathbf{q})$ of the intersite coupling I_{ij} at the ordering vector $\mathbf{q}$ where $I(\mathbf{q})$ is at its maximum. In a singlet ground state system with a Γ_1-Γ_6 splitting energy Δ a spontaneous induced moment can only appear when the control parameter ξ is larger than 1, with $\xi = 2\alpha^2\, I_e/\Delta$ [64,66] and $\alpha^2 = \sum_\sigma |\langle\Gamma_1|J_x|\Gamma_{6,\sigma}\rangle|^2$, where σ is the degeneracy index of the Γ_6 states, with numerical value $\alpha = 3.1$. The saturation moment at zero temperature then is given by $m_0/(g_J\mu_B) = \langle J_x\rangle_0 = \alpha\xi^{-1}(\xi^2 - 1)^{1/2}$ ($g_J = 0.8$) which vanishes when approaching the critical value from above $\xi \to 1^+$, and becomes equal to $\langle J_x\rangle_0 = \alpha$, that of a quasidegenerate Γ_1-Γ_6 system, when $\xi \gg 1$, i.e., where the effective exchange strongly dominates over the splitting. In UGa_2 the moment of 3 μ_B / U is close to the latter case of the exchange dominated regime. See also Appendix A 4.

The thermal occupation of higher levels has to be considered for the determination of the temperature dependence of $\langle J_x\rangle_T$ and T_c as a function of the exchange I_e and CF splitting Δ. This can be done within our full multiplet calculation (including all angular momentum multiplets J and their respective CF multiplets) by solving iteratively the self-consistency equation $\langle J_{x,y}\rangle_T = \sum_n p_n\langle n|J_{x,y}|n\rangle$ where $E_n(\langle J_{x,y}\rangle_T)$ and $|n\rangle(\langle J_{x,y}\rangle_T)$ are the eigenenergies and eigenstates in the presence of the molecular field $I_e\langle J_{x,y}\rangle_T$ for the given values of multiplet model parameters. Here $p_n{=}Z^{-1}\exp(-E_n/T)$ with $Z = \sum_m \exp(-E_m/T)$ are the thermal level occupations. The saturation moment $m_0/\mu_B = g_J\langle J_x\rangle_0$ may then be plotted as function of the splitting Δ and exchange I_e as shown in Fig. 5. Here the CF parameters from Ref. [25] (apart from the off-diagonal A_6^6) are scaled to modify the splitting Δ. It would be interesting to measure Δ using Raman spectroscopy [69]. For $\Delta = 3.3$ meV and $I_e = 1.78$ meV,

corresponding to $m_0(\Delta, I_e) \approx 3\ \mu_B$ (one point on the white line in Fig. 5), we obtain $T_c \approx 125$ K, in agreement with experiment. For completeness, we finally examine the impact of the self-consistent molecular field with I_e=1.78 meV on the RIXS [see Fig. 3(b)] and NIXS [see Fig. 4(a)] spectra. Here the CEF scheme giving $\Delta = 3.3$ meV and the Boltzmann population of excited states is also considered. We see that the molecular field has little impact on the spectra since, although mixed, the Γ_1 and Γ_6 show very similar lineshapes by themselves.

V. CONCLUSION

In summary, with tender RIXS at the U M_5 edge and hard x-ray NIXS at the U $O_{4,5}$ edge we have unveiled the U $5f^2$ multiplets inUGa_2 and shown that the magnetism is determined by the U $5f^2$ configuration with a Γ_1 singlet ground state and a Γ_6 doublet nearby. UGa_2, therefore, classifies as a quantum magnet. The origin of the induced magnetic order is due to the nondiagonal mixing of Γ_1 with excited Γ_6 states due to the effective intersite exchange coupling below T_c.

ACKNOWLEDGMENTS

All authors thank C. Geibel and A. C. Lawson for fruitful discussions, and acknowledge DESY (Hamburg, Germany), a member of the Helmholtz Association HGF, for the provision of experimental facilities. A.S. and A.A. benefited from support of the German Research Foundation (DFG), Project No. 387555779. L.H. and A.V.A. benefited from support of the Czech Science Foundation, Project No. 21-09766S.

APPENDIX

1. f^3 RIXS simulation with different values of the reduction factors

Figure 6 shows simulated f^3 RIXS spectra with $5f$-$5f$ Slater integral reduced of 45%, 40%, and 75%. The spectra are calculated with incident energies $h\nu_1$, $h\nu_2$, and $h\nu_3$, and with the crystal-field parameters from Ref. [23].

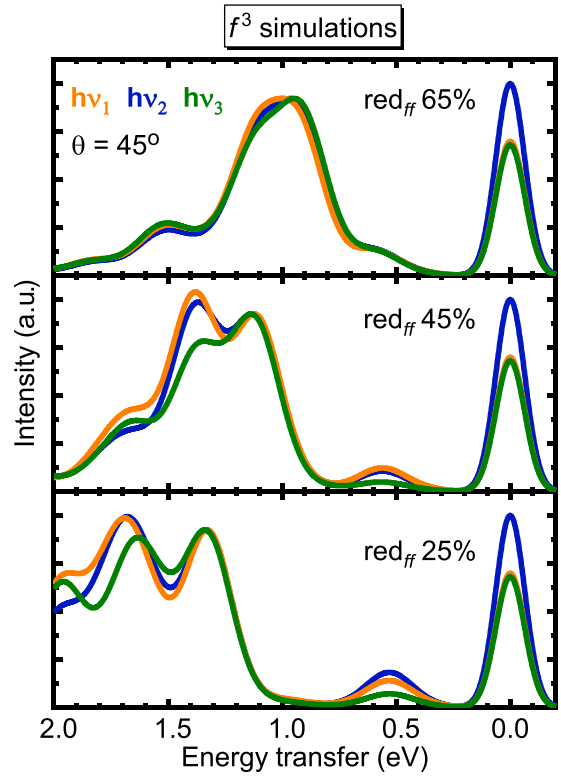

FIG. 6. Ionic f^3 simulated RIXS for different values of the $5f$-$5f$ reduction factors.

2. f^3 isotropic NIXS simulation with different values of the reduction factors

Figure 7 shows simulated f^3 NIXS spectra with $5f$-$5f$ and $5d$-$5f$ Slater integral reduction to 60%, 80%, and 100%. The crystal-field is not included in the calculations.

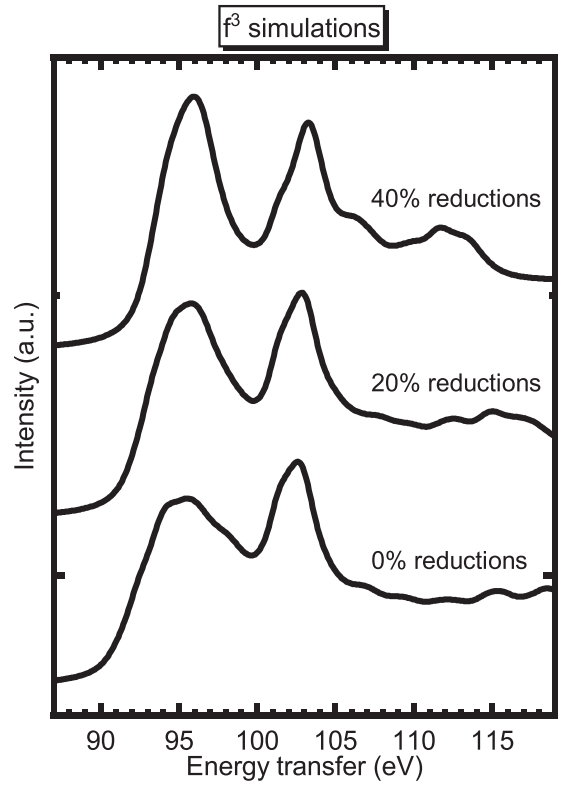

FIG. 7. Ionic f^3 simulated isotropic NIXS for different values of the $5f$-$5f$ and $5d$-$5f$ reduction factors.

3. Crystal-field parameters and ground state symmetry

Table I summarizes the crystal-field parameters and the corresponding ground state symmetries used in the RIXS calculations. For the Γ_5 states the relative $J_z = |\pm 4\rangle$ and $J_z = |\mp 2\rangle$ contribution is specified. The parameters giving a Γ_1 ground state are taken from Ref. [25].

4. Basics of induced moment magnetism

In this work the magnetism of UGa_2 is interpreted in terms of a localized model consisting of $5f$ CEF states for J=4. The on-site exchange interaction (resulting from Anderson-type

TABLE I. Crystal-field parameters in Wybourne notation and the corresponding ground state symmetries. For the Γ_5 states the J_z admixture is also specified.

GS symmetry	A_2^0 (K)	A_4^0 (K)	A_6^0 (K)	A_6^6 (K)
Γ_1	−220	680	−100	1040
Γ_6	−1044.41	696.272	−1856.72	−812.317
Γ_3	−365.543	−731.085	417.763	−731.085
Γ_4	−292.434	−841.328	300.557	731.085
Γ_5^1 $0.991\|\pm4\rangle + 0.128\|\mp2\rangle$	438.651	877.302	501.315	−877.302
Γ_5^2 $0.075\|\pm4\rangle - 0.997\|\mp2\rangle$	−626.644	−584.868	−313.322	522.204

on-site hybridization and Coulomb repulsion) between conduction and f-electron is assumed to have been eliminated leading to an effective RKKY interaction I_{ij} between $5f$ states on different sites i, j. I_e is the Fourier transform $I(\mathbf{q})$ of the intersite coupling I_{ij} at the ordering vector $\mathbf{q}$ where $I(\mathbf{q})$ is at its maximum. Restricting to FM with $\mathbf{q} = 0$ and to nearest neighbor terms only, the effective interaction is given by $I_e = zI_{nn}$ ($z =$ coordination number). If the $5f$ ground state were degenerate and carried an effective moment (i.e., having nonzero matrix elements of $\mathbf{J}$ within the multiplet) a quasiclassical ferromagnetic order would appear for any size of I_e where moments are simply aligned at a temperature $T_C \sim I_e$. Here, however, the lowest $5f$ states are nonmagnetic singlet Γ_1 ground state and Γ_6 doublet excited state at energy Δ. Due to their absent moments the FM order in UGa_2 can only appear through a more subtle mechanism called "induced order." This mechanism is well established for several $4f$ Pr and $5f$ U compounds with nonmagnetic low lying CEF states as in the present case. We refer to previous Refs. [64,66,70–74] for the detailed discussion of the subject. Although the Γ_1, Γ_6 states do not carry a moment there are *nondiagonal* matrix elements $\alpha/\sqrt{2} = \langle\Gamma_1|J_x|\Gamma_{6\sigma}\rangle$ ($\sigma = 1, 2$) of in-plane dipolar moment J_x (and similar for J_y) connecting them across the CEF gap Δ. This means that n.n. intersite interaction terms like $I_{ij}J_x(i)J_x(j)$ are able to mix the excited state Γ_6 into the noninteracting ground state Γ_1 and form spontaneously a new magnetic ground state at each site which is a superposition $|\Gamma_1'\rangle = u|\Gamma_1\rangle + v|\Gamma_6\rangle$ (and similar for the excited state). In this way the ground state moment appearance and its ordering happens simultaneously. The size of the ordered moment is then $\langle J_x\rangle = 2uv\alpha(n_1' - n_6')$ where $n_{1,6}'$ denote the thermal occupations of the CEF states which also depend on $\langle J_x\rangle$. This represents a molecular field equation for the induced moment $\langle J_x\rangle$. When temperature is lowered the occupation difference increases which may lead to a nonzero induced moment, provided the prefactor in the above equation is sufficiently large. This can be evaluated as a condition for the control parameter $\xi = 2\alpha^2 I_e/\Delta > 1$ to achieve a finite T_C and a saturation moment at $T = 0$ given by $\langle J_x\rangle_0 = \alpha\xi^{-1}(\xi^2 - 1)^{\frac{1}{2}}$. At zero temperature varying ξ across the quantum critical point (QCP) $\xi = 1$ we obtain a quantum phase transition from the paramagnetic ($\xi < 1$) to the (ferro-)magnetic ($\xi > 1$) state. In particular close to the QCP the induced moment quantum magnetism shows anomalous dependence of small saturation moment and low ordering temperature on the control parameter and is quite different from the quasiclassical magnetism where the influence of quantum fluctuations on moment and transition temperature is moderate.

[1] C. Pfleiderer, Rev. Mod. Phys. **81**, 1551 (2009).

[2] P. M. Oppeneer, J. Rusz, S. Elgazzar, M.-T. Suzuki, T. Durakiewicz, and J. A. Mydosh, Phys. Rev. B **82**, 205103 (2010).

[3] J. A. Mydosh and P. M. Oppeneer, Rev. Mod. Phys. **83**, 1301 (2011).

[4] R. Joynt and L. Taillefer, Rev. Mod. Phys. **74**, 235 (2002).

[5] S. Ran, C. Eckberg, Q.-P. Ding, Y. Furukawa, T. Metz, S. R. Saha, I.-L. Liu, M. Zic, H. Kim, J. Paglione, and N. P. Butch, Science **365**, 684 (2019).

[6] S. Ran, I.-L. Liu, Y. S. Eo, D. J. Campbell, P. M. Neves, W. T. Fuhrman, S. R. Saha, C. Eckberg, H. Kim, D. Graf, F. Balakirev, J. Singleton, J. Paglione, and N. P. Butch, Nat. Phys. **15**, 1250 (2019).

[7] L. Jiao, S. Howard, S. Ran, Z. Wang, J. O. Rodriguez, M. Sigrist, Z. Wang, N. P. Butch, and V. Madhavan, Nature (London) **579**, 523 (2020).

[8] I. M. Hayes, D. S. Wei, T. Metz, J. Zhang, Y. S. Eo, S. Ran, S. R. Saha, J. Collini, N. P. Butch, D. F. Agterberg, A. Kapitulnik, and J. Paglione, Science **373**, 797 (2021).

[9] M. Sato and Y. Ando, Rep. Prog. Phys. **80**, 076501 (2017).

[10] K. Haule and G. Kotliar, Nat. Phys. **5**, 796 (2009).

[11] H.-H. Kung, R. E. Baumbach, E. D. Bauer, V. K. Thorsmølle, W.-L. Zhang, K. Haule, J. A. Mydosh, and G. Blumberg, Science **347**, 1339 (2015).

[12] L. Miao, S. Liu, Y. Xu, E. C. Kotta, C.-J. Kang, S. Ran, J. Paglione, G. Kotliar, N. P. Butch, J. D. Denlinger, and L. A. Wray, Phys. Rev. Lett. **124**, 076401 (2020).

[13] R. Osborn, K. McEwen, E. Goremychkin, and A. Taylor, Phys. B: Condens. Matter **163**, 37 (1990).

[14] M. D. Le, K. A. McEwen, M. Rotter, J. Jensen, R. I. Bewley, T. Guidi, and D. Fort, J. Phys.: Condens. Matter **24**, 036002 (2012).

[15] E. S. Makarov and V. A. Ledvik, Sov. Phys. Cryst. **1**, 506 (1956).
[16] H. H. Hill, in *Plutonium 1970 and other Actinides*, edited by W. N. Miner (The Metallurgical Society of the AIME, New York, 1970), p. 2.
[17] A. Andreev, K. P. Belov, A. Deryagin, R. Z. Levitin, and A. Menovsky, J. Phys.Colloques **40**, C4-82 (1979).
[18] A. Lawson, A. Williams, J. Smith, P. Seeger, J. Goldstone, J. O'Rourke, and Z. Fisk, J. Magn. Magn. Mater. **50**, 83 (1985).
[19] A. V. Andreev, K. P. Belov, A. V. Deryagin, Z. A. Kazeï, R. Z. Levitin, A. Meňovský, Yu. F. Popov, and V. I. Silant'ev, Zh. Eksp. Teor. Fiz. **75**, 2351 (1978) [Sov. Phys. JETP **48**, 1187 (1978)].
[20] T. Honma, Y. Inada, R. Settai, S. Araki, Y. Tokiwa, T. Takeuchi, H. Sugawara, H. Sato, K. Kuwahara, M. Yokoyama, H. Amitsuka, T. Sakakibara, E. Yamamoto, Y. Haga, A. Nakamura, H. Harima, H. Yamagami, and Y. Ōnuki, J. Phys. Soc. Jpn. **69**, 2647 (2000).
[21] A. V. Kolomiets, J.-C. Griveau, J. Prchal, A. V. Andreev, and L. Havela, Phys. Rev. B **91**, 064405 (2015).
[22] Y. Kuroiwa, M. Kohgi, T. Osakabe, N. Sato, and Y. Ōnuki, *Proceedings of the Fifth International Symposium Advance Nuclear Energy Research*, JAERI-M 93-228 (pt. 2) (1993), p. 314.
[23] R. Radwański and N. Kim-Ngan, J. Magn. Magn. Mater. **140-144**, 1373 (1995).
[24] M. Diviš, M. Richter, H. Eschrig, and L. Steinbeck, Phys. Rev. B **53**, 9658 (1996).
[25] M. Richter, M. Diviš, J. Forstreuter, K. Koepernik, L. Steinbeck, and H. Eschrig, Phys. B: Condens. Matter **230-232**, 519 (1997).
[26] B. Chatterjee and J. Kolorenč, Phys. Rev. B **103**, 205146 (2021).
[27] S.-i. Fujimori, M. Kobata, Y. Takeda, T. Okane, Y. Saitoh, A. Fujimori, H. Yamagami, Y. Haga, E. Yamamoto, and Y. Ōnuki, Phys. Rev. B **99**, 035109 (2019).
[28] A. V. Kolomiets, M. Paukov, J. Valenta, B. Chatterjee, A. V. Andreev, K. O. Kvashnina, F. Wilhelm, A. Rogalev, D. Drozdenko, P. Minarik, J. Kolorenč, M. Richter, J. Prchal, and L. Havela, Phys. Rev. B **104**, 045119 (2021).
[29] W.-D. Schneider and C. Laubschat, Phys. Rev. Lett. **46**, 1023 (1981).
[30] T. Gouder, L. Havela, M. Diviš, J. Rebizant, P. Oppeneer, and M. Richter, J. Alloys Compd. **314**, 7 (2001).
[31] K. O. Kvashnina, S. M. Butorin, D. K. Shuh, K. Ollila, I. Soroka, J.-H. Guo, L. Werme, and J. Nordgren, Lawrence Berkeley National Laboratory, 2008, https://escholarship.org/uc/item/15c2r4hn.
[32] S. M. Butorin, in *Actinide Nanoparticle Research*, edited by S. N. Kalmykov and M. A. Denecke (Springer, Berlin, Heidelberg, 2011), pp. 63–103.
[33] S. M. Butorin, D. K. Shuh, K. O. Kvashnina, J. Guo, L. Werme, and J. Nordgren, Anal. Chem. **85**, 11196 (2013).
[34] L. A. Wray, J. Denlinger, S.-W. Huang, H. He, N. P. Butch, M. B. Maple, Z. Hussain, and Y.-D. Chuang, Phys. Rev. Lett. **114**, 236401 (2015).
[35] S. Liu, Y. Xu, E. C. Kotta, L. Miao, S. Ran, J. Paglione, N. P. Butch, J. D. Denlinger, Y.-D. Chuang, and L. A. Wray, Phys. Rev. B **106**, L241111 (2022).
[36] G. H. Lander, M. Sundermann, R. Springell, A. C. Walters, A. Nag, M. Garcia-Fernandez, K. J. Zhou, G. van der Laan, and R. Caciuffo, J. Phys.: Condens. Matter **33**, 06LT01 (2021).
[37] A. Amorese, A. Severing, A. Walters, and K. Zhou (private communication).
[38] A. Amorese, A. Severing, K. Kummer, and N. B. Brookes (private communication).
[39] K. O. Kvashnina, H. C. Walker, N. Magnani, G. H. Lander, and R. Caciuffo, Phys. Rev. B **95**, 245103 (2017).
[40] A. Amorese, G. Dellea, M. Fanciulli, S. Seiro, C. Geibel, C. Krellner, I. P. Makarova, L. Braicovich, G. Ghiringhelli, D. V. Vyalikh, N. B. Brookes, and K. Kummer, Phys. Rev. B **93**, 165134 (2016).
[41] N. Brookes, F. Yakhou-Harris, K. Kummer, A. Fondacaro, J. Cezar, D. Betto, E. Velez-Fort, A. Amorese, G. Ghiringhelli, L. Braicovich, R. Barrett, G. Berruyer, F. Cianciosi, L. Eybert, P. Marion, P. van der Linden, and L. Zhang, Nucl. Instrum. Methods Phys. Res. Sect. A **903**, 175 (2018).
[42] A. Amorese, K. Kummer, N. B. Brookes, O. Stockert, D. T. Adroja, A. M. Strydom, A. Sidorenko, H. Winkler, D. A. Zocco, A. Prokofiev, S. Paschen, M. W. Haverkort, L. H. Tjeng, and A. Severing, Phys. Rev. B **98**, 081116(R) (2018).
[43] A. Amorese, O. Stockert, K. Kummer, N. B. Brookes, D.-J. Kim, Z. Fisk, M. W. Haverkort, P. Thalmeier, L. H. Tjeng, and A. Severing, Phys. Rev. B **100**, 241107(R) (2019).
[44] M. Nakazawa, S. Tanaka, T. Uozumi, and A. Kotani, J. Phys. Soc. Jpn. **65**, 2303 (1996).
[45] S. M. Butorin, D. C. Mancini, J.-H. Guo, N. Wassdahl, J. Nordgren, M. Nakazawa, S. Tanaka, T. Uozumi, A. Kotani, Y. Ma, K. E. Myano, B. A. Karlin, and D. K. Shuh, Phys. Rev. Lett. **77**, 574 (1996).
[46] C. Dallera, K. Giarda, G. Ghiringhelli, A. Tagliaferri, L. Braicovich, and N. B. Brookes, Phys. Rev. B **64**, 153104 (2001).
[47] H. Gretarsson, D. Ketenoglu, M. Harder, S. Mayer, F.-U. Dill, M. Spiwek, H. Schulte-Schrepping, M. Tischer, H.-C. Wille, B. Keimer, and H. Yavaş, J. Synchrotron Rad. **27**, 538 (2020).
[48] A. H. Said, T. Gog, M. Wieczorek, X. Huang, D. Casa, E. Kasman, R. Divan, and J. H. Kim, J. Synchrotron Rad. **25**, 373 (2018).
[49] W. Schülke, *Electron Dynamics by Inelastic X-ray Scattering*, Oxford Series on Synchrotron Radiation (Oxford University Press, Oxford, 2007).
[50] M. W. Haverkort, A. Tanaka, L. H. Tjeng, and G. A. Sawatzky, Phys. Rev. Lett. **99**, 257401 (2007).
[51] R. A. Gordon, G. T. Seidler, T. T. Fister, M. W. Haverkort, G. A. Sawatzky, A. Tanaka, and T. K. Sham, Europhys. Lett. **81**, 26004 (2008).
[52] J. A. Bradley, S. Sen Gupta, G. T. Seidler, K. T. Moore, M. W. Haverkort, G. A. Sawatzky, S. D. Conradson, D. L. Clark, S. A. Kozimor, and K. S. Boland, Phys. Rev. B **81**, 193104 (2010).
[53] R. Caciuffo, G. van der Laan, L. Simonelli, T. Vitova, C. Mazzoli, M. A. Denecke, and G. H. Lander, Phys. Rev. B **81**, 195104 (2010).
[54] S. Sen Gupta, J. A. Bradley, M. W. Haverkort, G. T. Seidler, A. Tanaka, and G. A. Sawatzky, Phys. Rev. B **84**, 075134 (2011).
[55] M. Sundermann, K. Chen, H. Yavaş, H. Lee, Z. Fisk, M. W. Haverkort, L. H. Tjeng, and A. Severing, Europhys. Lett. **117**, 17003 (2017).
[56] M. W. Haverkort, J. Phys.: Conf. Ser. **712**, 012001 (2016).
[57] R. D. Cowan, *The Theory of Atomic Structure and Spectra* (University of California Press, Berkeley and Los Angeles, 1981).
[58] A. Tanaka and T. Jo, J. Phys. Soc. Jpn. **63**, 2788 (1994).

[59] F. de Groot and A. Kotani, *Core Level Spectroscopy of Solids*, Advances in Condensed Matter Science Vol. 6 (CRC Press, Boca Raton, 2008).
[60] S. Agrestini, C.-Y. Kuo, M. Moretti Sala, Z. Hu, D. Kasinathan, K.-T. Ko, P. Glatzel, M. Rossi, J.-D. Cafun, K. O. Kvashnina, A. Matsumoto, T. Takayama, H. Takagi, L. H. Tjeng, and M. W. Haverkort, Phys. Rev. B **95**, 205123 (2017).
[61] A. Kotani and S. Shin, Rev. Mod. Phys. **73**, 203 (2001).
[62] G. Khaliullin, Phys. Rev. Lett. **111**, 197201 (2013).
[63] A. Jain, M. Krautloher, J. Porras, G. H. Ryu, D. P. Chen, D. L. Abernathy, J. T. Park, A. Ivanov, J. Chaloupka, G. Khaliullin, B. Keimer, and B. J. Kim, Nat. Phys. **13**, 633 (2017).
[64] P. Thalmeier, Phys. Rev. B **103**, 144435 (2021).
[65] L. Miao, R. Basak, S. Ran, Y. Xu, E. Kotta, H. He, J. D. Denlinger, Y.-D. Chuang, Y. Zhao, Z. Xu, J. W. Lynn, J. R. Jeffries, S. R. Saha, I. Giannakis, P. Aynajian, C.-J. Kang, Y. Wang, G. Kotliar, N. P. Butch, and L. A. Wray, Nat. Commun. **10**, 644 (2019).
[66] P. Thalmeier, Eur. Phys. J. B **27**, 29 (2002).
[67] P. Thalmeier and G. Zwicknagl, *Unconventional Superconductivity and Magnetism in Lanthanide and Actinide Intermetallic Compounds* (Elsevier, Amsterdam, 2005), p. 135.
[68] A. Amorese, M. Sundermann, B. Leedahl, A. Marino, D. Takegami, H. Gretarsson, A. Gloskovskii, C. Schlueter, M. W. Haverkort, Y. Huang, M. Szlawska, D. Kaczorowski, S. Ran, M. B. Maple, E. D. Bauer, A. Leithe-Jasper, P. Hansmann, P. Thalmeier, L. H. Tjeng, and A. Severing, Proc. Natl. Acad. Sci. USA **117**, 30220 (2020).
[69] J. Buhot, M.-A. Méasson, Y. Gallais, M. Cazayous, A. Sacuto, G. Lapertot, and D. Aoki, Phys. Rev. Lett. **113**, 266405 (2014).
[70] B. Grover, Phys. Rev. **140**, A1944 (1965).
[71] B. R. Cooper, Phys. Rev. B **6**, 2730 (1972).
[72] R. J. Birgeneau, J. Als-Nielsen, and E. Bucher, Phys. Rev. B **6**, 2724 (1972).
[73] W. J. L. Buyers, T. M. Holden, and A. Perreault, Phys. Rev. B **11**, 266 (1975).
[74] J. Jensen and A. R. Mackintosh, *Rare Earth Magnetism* (Clarendon Press, Oxford, 1991).